Exp.-Nr. A2-10/05
Eingang: 26.08.05
an PAC:

Mainz Microtron MAMI

Collaboration A2: "Real Photons"
Spokesperson: A. Thomas

Proposal for an Experiment

**" Photoproduction of η-mesons off the neutron –
Part I: angular distributions and double polarization observable E"**

Collaborators :

CrystalBall@MAMI collaboration

Spokespersons for the Experiment :
B. Krusche, University of Basel, Basel, Switzerland
W. Briscoe, The George Washington University, Washington DC, USA

Abstract of Physics :

We propose to measure η-photoproduction from the neutron in particular in the energy range around 1 GeV incident photon energy (corresponding to W≈1.675 GeV). Previous experiments have shown a clear structure in the excitation function in this energy region, which is not seen in the excitation function of the proton. In the MAID model, a similar enhancement of the neutron cross section is found, which in the model is due to the excitation of the $D_{15}(1675)$ resonance. However, our preliminary angular distributions are not in agreement with the model. Here, we propose to re-measure the angular distributions with much better precision and to measure the double polarization observable E, which has a large sensitivity to the D_{15} resonance.

Abstract of Equipment :

We require the 4π electromagnetic calorimeter consisting of the Crystal Ball and TAPS detectors. The wire chambers and the PID detector are needed for the separation of recoil protons and neutrons going into the Crystal Ball detector. The measurement of the angular distributions requires an unpolarized photon beam on a liquid deuterium target. The measurement of the GDH observable E requires a circularly polarized beam on a longitudinally polarized deuteron (deuterated butanol target).

MAMI–Specifications :

beam energy	1500 MeV
beam current	< 100nA
time structure	cw
polarization	unpolarized and circularly polarized photons

Experiment–Specifications :

experimental hall/beam	A2
detector	Crystal Ball, TAPS, MWPC, PID
target material	liquid deuterium, polarized deuterated butanol

Beam Time Request :

set–up/tests with beam	24 hours
data taking	200 hours (liquid deuterium target) (???parallel with proposal A2/ ???)
data taking	700 hours (frozen spin target) (???parallel with proposal A2/ ???)

Preface

The two proposals: Photoproduction of η-mesons from the neutron:

Part I: angular distributions and double polarization observable E
Part II: photon beam asymmetry and double polarization observable G

deal with the same physics. Therefore the introduction, motivation and discussion of the physics case (sections 1.1 -3) for η photoproduction are identical in the two proposals. The proposals differ in the description of the experimental setups and beam requirements (subsection 3.1). The MAMI C proposal, as a side aspect, aims also at the study of η' photoproduction from the deuteron at threshold, which, however, does not require additional beam time. The proposals are independently submitted since one part of the measurements (angular distributions and double polarization observable E) is proposed for the MAMI C facility in Mainz and the other part (photon beam asymmetry and double polarization observable G) is proposed for the ELSA facility in Bonn. As discussed below, in this way the respective advantages of the two facilities can be used in an optimal way. Since the two parts of the experiment will be done in the framework of different experimental collaborations (CBELSA/TAPS in Bonn and Crystal Ball/TAPS in Mainz) two separate proposals are submitted.

1 Photoproduction of η mesons off the neutron

1.1 Introduction and Motivation

The excitation spectrum of baryons is intimately connected to the properties of QCD in the low-energy regime, where it cannot be treated in perturbative approaches. Originally, most experimental information on the baryon spectrum was obtained from hadron induced reactions, in particular from pion-nucleon scattering. However, during the last decade or so, photon induced meson production reactions on the proton have largely contributed to this field. At the modern facilities (ELSA in Bonn, GRAAL in Grenoble, JLAB in Newport News, MAMI in Mainz and Spring8 in Osaka) mainly two strategies have been followed. Different reactions have been explored to search for 'missing resonances' over large regions of excitation energy and precision experiments have been performed on the properties of lower lying resonances. At the Mainz and Bonn facilities, the next generation of experiments will largely profit from the availability of linearly and circularly polarized photon beams combined with polarized targets, so that the rich information provided by double polarization experiments becomes available. This will allow a much more efficient investigation of resonance properties since one may select for any resonance of interest the most sensitive combination of experimental observables.

Although experimental programs for the study of nucleon resonances off the proton via photoproduction of mesons are well developed, so far much less effort has gone into the investigation of the corresponding reactions on the neutron. Photoproduction of mesons off the neutron serves two different purposes. First, this is the only possibility to disentangle the isospin structure of the electromagnetic resonance excitations, which serves as one stringent test of baryon model predictions. Secondly, in some cases the electromagnetic coupling of resonances to the neutron ground state may be much stronger than in the proton case, so that certain resonances potentially can be studied in more detail on the neutron.

The investigation of photoproduction reactions off the neutron is of course complicated by the non-availability of free neutron targets, which requires the use of light nuclei as target materials. The deuteron with its low binding energy is clearly the best target choice for most measurements on the neutron. However, the measurement off bound neutrons does not only smear excitation functions and kinematical observables due to the momentum distribution of the nucleons, it also introduces additional uncertainties due to nuclear effects like final state interaction (FSI) or interferences terms. The actual importance of such nuclear effects may be very different for different meson production reactions. Substantial effects have been found for example in the photoproduction of π^o mesons off the deuteron in the Δ-resonance region and in the second resonance region. In the first case the measured cross sections [1] could only be understood [2] when FSI (in particular NN FSI) was thoroughly treated in the models. The experimental results of inclusive π^o photoproduction in the second resonance region are even still not fully understood (see [3] for an overview). However, the situation is much more favorable for the photoproduction of η mesons, which is the topic of this proposal.

Quasifree and coherent photoproduction of η mesons off the deuteron, off ^{3}He, and off ^{4}He in the excitation range of the $S_{11}(1535)$ resonance has been studied during the last years in quite some detail [4, 5, 6, 7, 8, 9, 10] at different levels of sophistication. Inclusive experiments, have detected only the η-mesons but not the recoil nucleons. The measured cross sections could be consistently understood in the framework of simple PWIA models, which took into account the Fermi motion of the bound nucleons, when an approximately energy independent ratio $\sigma_n/\sigma_p \approx 2/3$ was assumed. In this case, the comparison of the results from ^{4}He and the deuteron (see [3] for an overview) provides a stringent test of possible model dependent effects, since the influence of the different nuclear momentum distributions in the loosely bound deuteron and the strongly bound ^{4}He nucleus is severe. The total cross sections from ^{4}He and from the deuteron are almost equal at incident photon energies around 800 MeV, although twice the number of

nucleons is involved in the He case. Nevertheless in both cases PWIA calculations with the 2/3 ratio of the free proton and neutron cross sections reproduces the data quite well. Also exclusive measurements with coincident detection of the recoil nuclei [5, 6, 9] are in agreement with this result. Typical cross section ratios from the exclusive measurements (see [3] for an

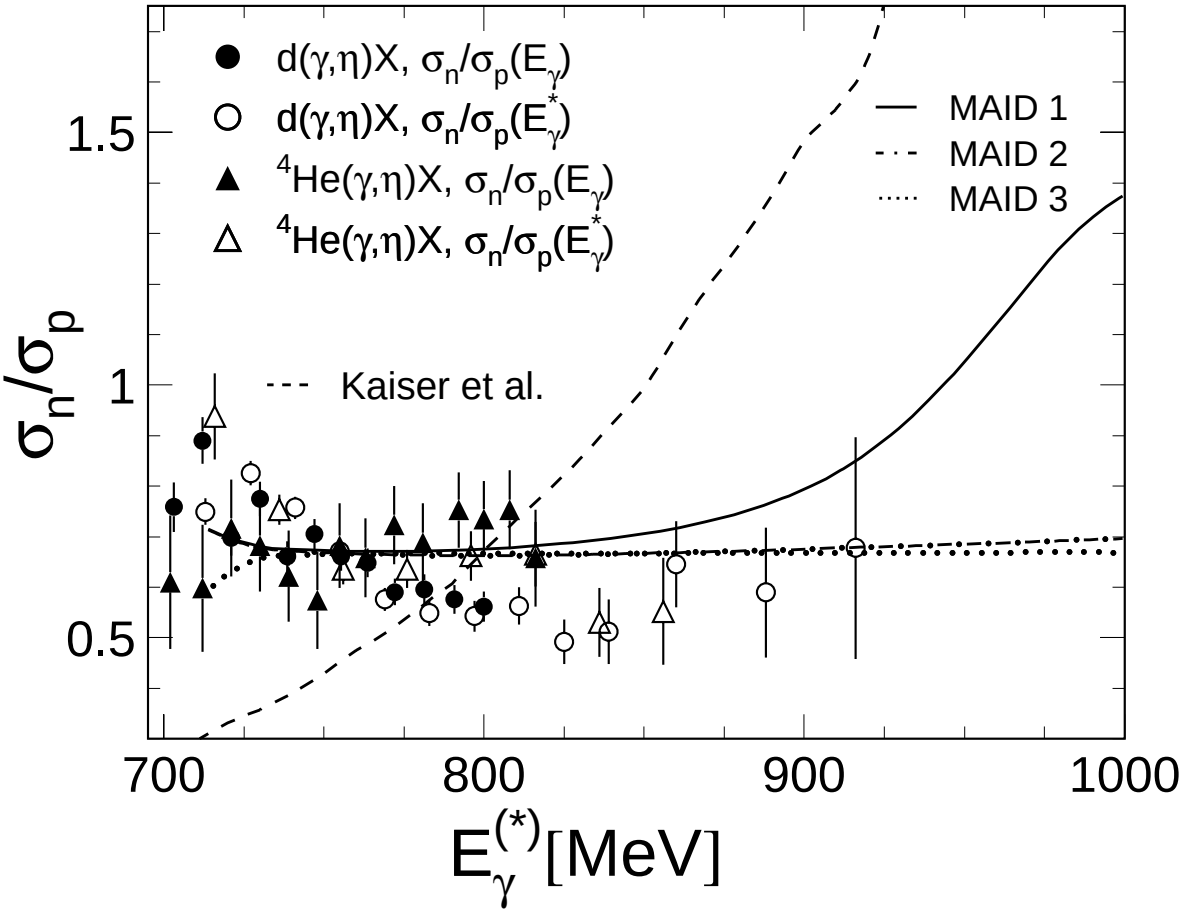

Figure 1: Measured ratio of the cross section of η photoproduction from the neutron and from the proton. Data are from obtained from deuteron and ^{4}He targets are from [9, 6]. Dashed curve: prediction from the $K\Sigma$ model of the $S_{11}(1535)$ (Kaiser et al. [11, 12]). The curves labeled MAID are the predictions from the MAID model [13] for the full model (MAID 1), the $S_{11}(1535)$-resonance, Born terms and vector meson exchange (MAID 2), and for the $S_{11}(1535)$ alone (MAID 3).

overview) are summarized in fig. 1. The data labeled with $E_\gamma^\star$ have been corrected for the momenta of the target nucleons derived from the complete kinematical determination of the final state (η and recoil nucleon) and the incident photon energy. Altogether, the results can be understood in simple plane wave approximations and FSI effects seem to play only a significant role in the vicinity of the production thresholds, which is not of interest for this proposal. The results, together with the measurements of coherent photoproduction of η mesons from light nuclei, have lead to a precise determination of the isospin structure of the excitation of the $S_{11}(1535)$ resonance [9]. Furthermore, it has specifically contributed to the discussion of the internal structure of this resonance. Kaiser et al. [11, 12] had suggested that this state does not correspond to a genuine three-quark structure but is more like a $K\Sigma$ nucleon-meson quasi-bound state. Their model reproduced the measured cross sections for $p(\gamma, p)\eta$ quite well, but it does not reproduce the neutron-proton cross section ratio (see fig.1).
At higher incident photon energy ($E_\gamma > 900$ MeV) models of η-photoproduction like the η-MAID model [13] predict a strong rise of the neutron - proton cross section ratio due to the

contribution of other nucleon resonances (see fig. 1). In the MAID model, the relative rise of he neutron cross section compared to the proton cross section which peaks at incident photon energies around 1 GeV, is mainly due to the excitation of the $D_{15}(1675)$ four star resonance. According to the review of particle properties (PDG) [14] this resonance has substantially larger photon couplings to the neutron than to the proton:

$$A^n_{1/2} = (-43 \pm 12) \cdot 10^3 \mathrm{GeV}^{-1/2} \quad (1)$$

$$A^n_{3/2} = (-58 \pm 13) \cdot 10^3 \mathrm{GeV}^{-1/2} \quad (2)$$

$$A^p_{1/2} = (+19 \pm 8) \cdot 10^3 \mathrm{GeV}^{-1/2} \quad (3)$$

$$A^p_{3/2} = (+15 \pm 9) \cdot 10^3 \mathrm{GeV}^{-1/2} \ . \quad (4)$$

In the framework of quark models there are predictions for a D_{15} resonance in this energy range with has a similar coupling pattern. A model which is based on single quark excitations from the nucleon ground state to the [70,1^-] multiplet [15] predicts rather small photon couplings to the proton, but larger ones to the neutron. On the other hand, the decay branching ratio into the $N\eta$ final state of this resonance is estimated by the PDG in the range 0 - 1 %, i.e. so far no significant contribution to η photoproduction is established. Also an analysis of photoproduction off the proton, including the most recent η photoproduction data in this energy range [16], finds only a very small contribution of this resonance and a ratio of the helicity couplings ($A^p_{1/2}/A^p_{3/2} = 0.06 \pm 0.18$), which is in contradiction to the PDG value ($A^p_{1/2}/A^p_{3/2} = 0.93 \pm 0.18$). In summary, so far the contribution of this resonance to η photoproduction is not settled and only precise data for quasifree photoproduction from the neutron can be expected to solve this question. The sensitivity of different observables to this resonance is discussed n detail in sections 1.2,1.3.

It is very interesting to note, that also in the framework of the chiral soliton model [17] a state is predicted in this energy range, with has much stronger photon couplings to the neutron than to the proton *and* a large decay branching ratio into $N\eta$. This state is the nucleon-like member of the predicted anti-decuplet of pentaquarks, which would be a P_{11} state. Exact $SU(3)_F$ would forbid the photoexcitation of the proton to the proton-like member of the anti-decuplet. But even after accounting for $SU(3)_F$ violation the chiral soliton model predicts [18] that the photoexcitaion of this state is suppressed on the proton and should mainly occur on the neutron. Kim et al. [19] have calculated the magnetic transitions moments for the anti-decuplet states and found a considerable enhancement for the excitation of the nucleon-like state on the neutron with respect to the proton. Also recent calculations [20] in a diquark picture of possible anti-decuplet states comes to a similar conclusion.

On the experimental side, recently the GRAAL collaboration [21] has reported preliminary results for quasifree η photoproduction off protons and off neutrons bound in the deuteron. The excitation functions for selected angular ranges are shown in fig. 2. The excitation functions of quasifree η production measured in coincidence with recoil protons shows a smooth behavior and agrees as expected with the results for the free proton at all incident photon energies not too close to the kinematical production threshold. However, on the neutron a relatively narrow structure is observed at incident photon energies around 1 GeV corresponding to $W \approx 1675$ MeV. At the same time also the photon beam asymmetry on the neutron shows a different behavior from the proton. From a simulation of a resonance structure, superimposed on a smooth background, Kutznetsov et al.[21], have extracted tentative values for the excitation energy and width of the visible structure as W=1675 MeV, Γ=40 MeV. Since the excitation function is smeared by the momentum distribution of the bound neutrons, the intrinsic width of the resonance like structure must be even smaller, more in the range of 10 MeV. This would be clearly not in agreement with the parameters of the $D_{15}(1675)$ resonance discussed above which has an estimated width of 130 - 165 MeV [14], although of course one has to be extremely careful with resonance parameters extracted from such a simple fit, which does e.g. not account for

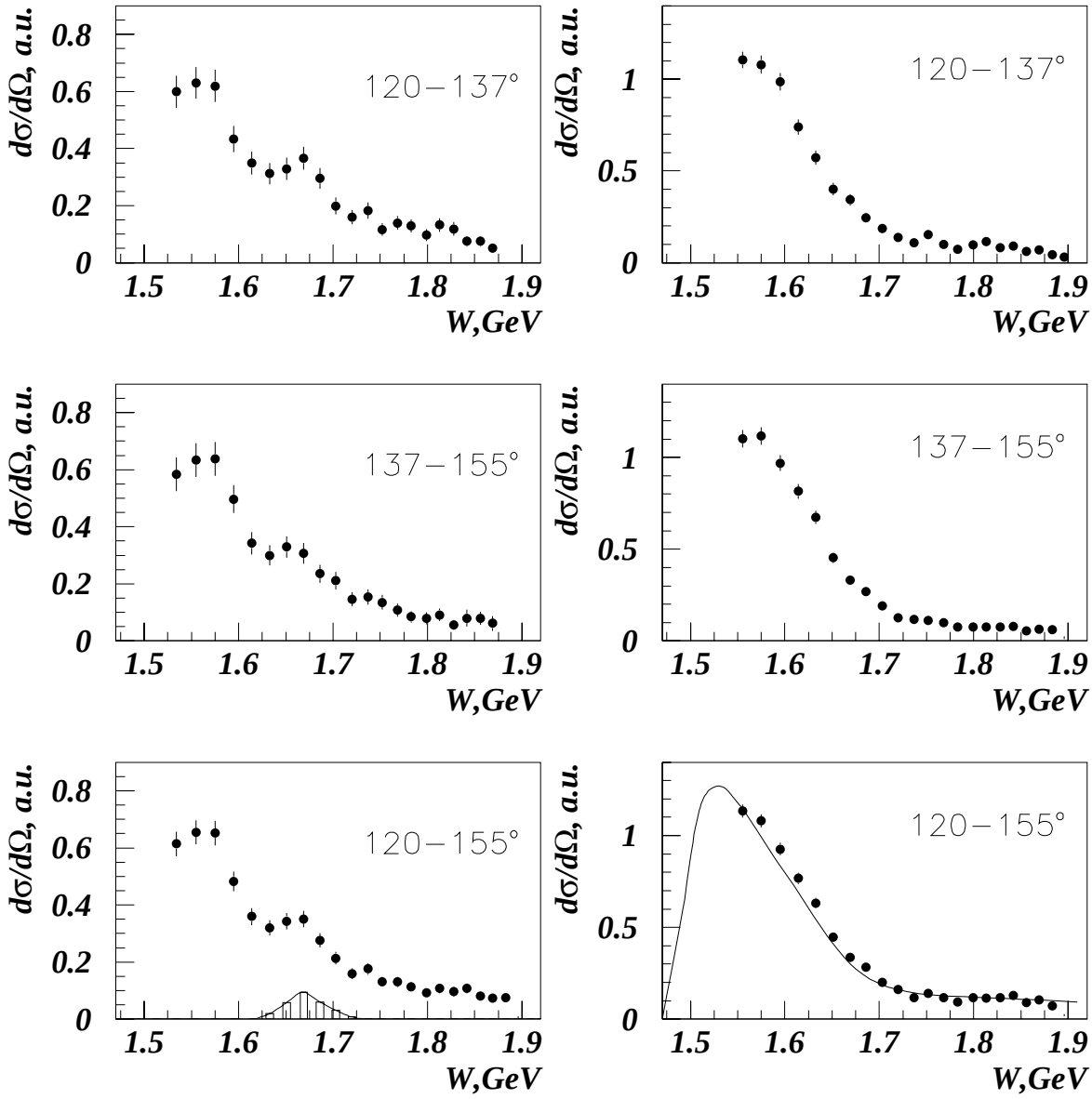

Figure 2: Preliminary results for quasifree η-photoproduction off the proton (right hand side) and off the neutron (left hand side) from the GRAAL experiment [21] using a deuterium target. The solid line for the proton data shows the SAID [22] result for the free proton cross section.

interference terms with background and other resonances. As discussed above, such a narrow structure is of course just what would be expected from the chiral quark soliton models for the nucleon like pentaquark state. Very recently, Azimov et al.[23] have approximated the radiative decay width of the structure in the GRAAL data and found good agreement with the ChQSM predictions [19].

However, with the very unclear status of pentaquark states, the situation is completely open, and explanations of the GRAAL structure by the excitation of conventional three-quark resonances like the $D_{15}(1675)$ is certainly not ruled out. It is therefore very urgent, to investigate quasifree η photoproduction on the neutron n this energy regions in more detail. In particular the measurement of observables, which can pin down the quantum numbers of this structure is very desirable. It should be pointed out, that of course also the case of a conventional three quark state that is excited so dominantly on the neutron is of high interest for baryon spectroscopy and would allow the precise determination of the properties of this state.

1.2 Preliminary results from previous ELSA experiments

Triggered by the prediction of the MAID model of strong contributions from higher lying resonances to η photoproduction off the neutron, we had previously submitted a proposal to measure angular distributions for this reaction with the CBELSA/TAPS setup in Bonn. The experiment was successfully done in 2003. Since at the time when the experiment was done, also linearly polarized beams at the photon energy of interest where available at the ELSA facility, in addition to excitation functions and angular distributions also the photon beam asymmetry could be measured. In the following we will discuss preliminary results from this experiments, which will be part of the PhD thesis of I. Jaegle, U. Basel.

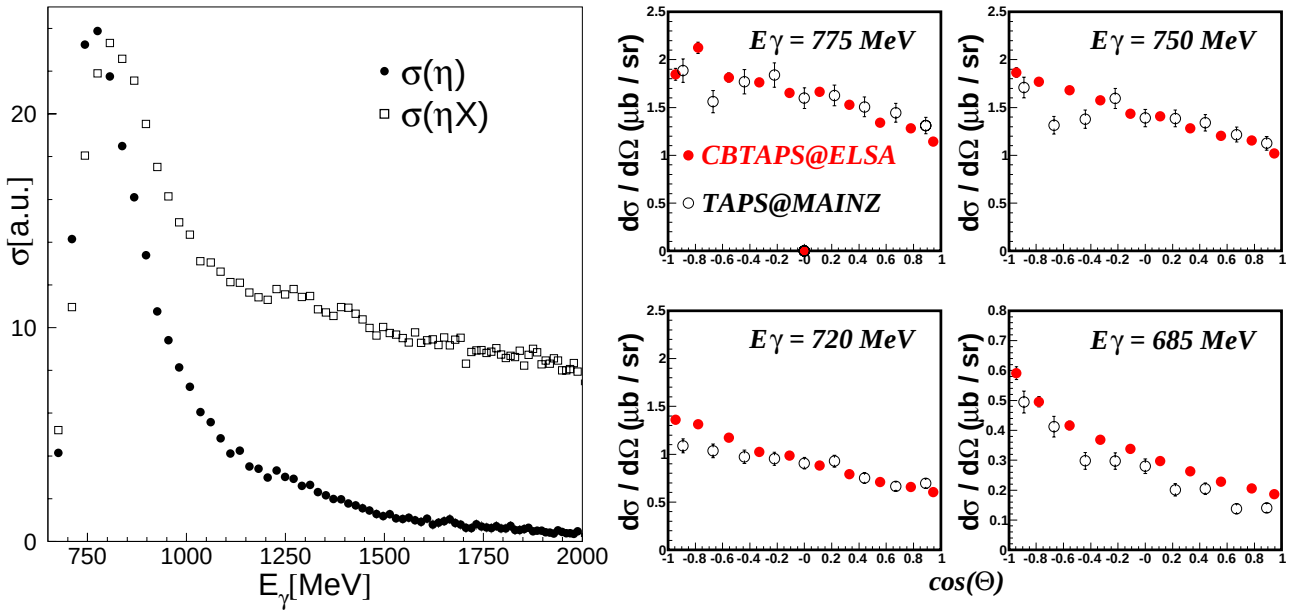

Figure 3: Left hand side: excitation functions for final states with at least one η and with one η and no further meson. Right hand side: inclusive η photoproduction on the deuteron at low incident photon energies compared to previous results [4].

In the experiment the $\eta \rightarrow 3\pi^o \rightarrow 6\gamma$ decay channel of the η meson was used. The decay photons have been identified in the barrel and in the TAPS forward wall with the standard analysis methods, using the inner detector of the barrel, the veto detector of TAPS, time-of-flight and pulse-shape techniques. Events with six photon clusters where than selected for further analysis. The six photons were combined into all disjunct combinations of thee pairs, and the invariant mass of the photon pairs was compared to the pion mass. Cuts were made on the invariant masses of the photon pairs and then the kinematical parameters of the three pions (after adjustion using the kinematical overdetermination) were used to calculate the invariant mass of the six-photon state. Typical invariant mass spectra are shown in the upper row of fig. 4 for three typical regions of incident photon energies and for reactions with coincident recoil protons and recoil neutrons. At low incident photon energies, they show basically background free invariant mass peaks of the η meson. At higher incident photon energies background mainly due o the $\eta\pi^o$ final state appears in the spectra. Background from the $\eta\pi$ final state is quite large at high incident photon energies. Cuts on the η invariant mass alone can of course not remove this background. Therefore in addition the kinematical overdetermination of the reaction is used for a missing mass analysis (the momentum distribution of the nucleons bound in the deuteron can be neglected, since it only results in a moderate broadening of the spectra. Typical missing mass spectra after a cut on the η invariant mass are shown in the lower part of fig. 4. The background in this spectra is mainly due to events where an additional pion in the final state escaped detection (e.g. charged pions that go along the beam tube).

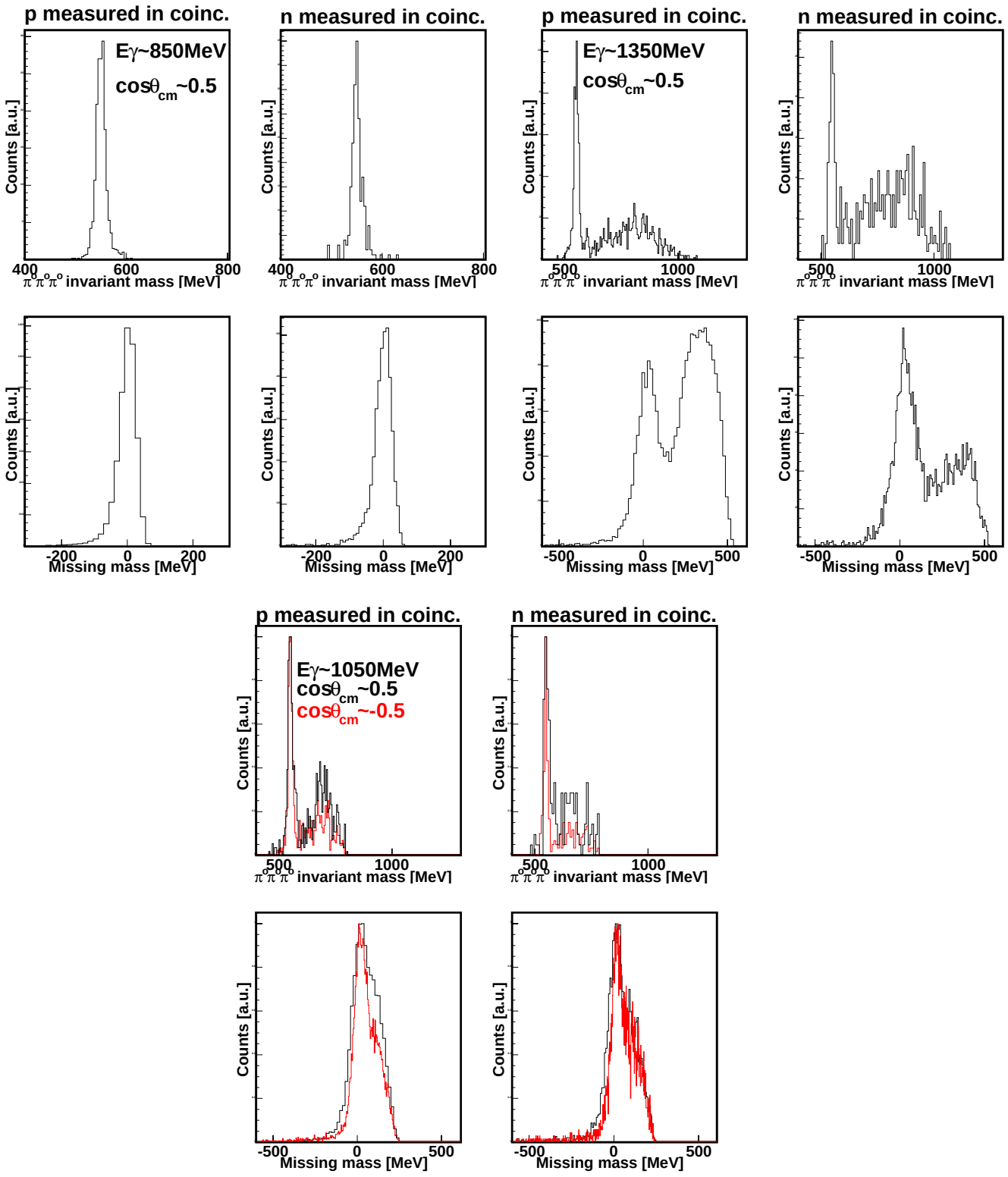

Figure 4: Invariant mass spectra and missing mass spectra for η photoproduction for three typical incident photon energies. For all three energy regions the upper parts show the invariant mass, the lower part the missing mass, the left columns correspond to reactions in coincidence with recoil protons, the right columns to recoil neutrons. For the most interesting energy region around 1 GeV incident photon energy spectra for two typical angular regions cos(Θ)=0.5 (black), cos(Θ)=-0.5 (red) are shown, for the other photon energies only the forward angles are shown.

This background is still moderate in the most interesting range around photon energies of 1 GeV, but becomes quite large at higher energies. For the preliminary results discussed below, a very conservative cut (missing mass from the peak to negative values) was used. This means a reduction of the 'good' events by roughly a factor of two, but eliminates the background almost completely.

As a first check of the data, the inclusive reaction without any condition for the recoil nucleons was analyzed. Excitation functions for the η final state (i.e. after kinematical cuts which remove $\eta\pi$ final states) and for the ηX final state are shown in fig. 3, left hand side. It is obvious, that the contribution from $\eta\pi$ is substantial. However, it can be suppressed almost completely with the kinematical cuts (see also fig. 7, comparison of quasifree proton cross section to MAID model). In the right hand side of the figure, angular distributions of the η final state are compared to previous results [4] in the low energy regime. The overall agreement is quite good.

In the next step, the exclusive reaction channels with identification of the recoil nucleons were analyzed. Differential cross sections for quasifree η production from the bound proton are compared in fig. 5 to the reaction on the free proton [16] (the absolute normalization of the data is not yet determined, it is scaled with one energy independent constant to the free proton data). Again the agreement is quite satisfactory. This indicates that in the energy range of interest, the influence of the momentum distribution of the bound nucleons on the angular distributions is small and no significant FSI effects are observed. The measured quasifree cross sections are thus a good approximation of the free nucleon cross section (the influence of Fermi motion could of course be de-folded in a more elaborate analysis). Data for the extreme forward angular region could not be measured, since η mesons at forward angles correspond to protons with low kinetic lab energies (<100 MeV), which cannot be detected (absorption in the target etc.). This problem does however not occur for recoil neutrons which can be detected at much lower kinetic energies (down to 25 MeV).

The angular distributions for the quasifree reaction off the neutron are compared to the quasifree proton data in fig. 6 (again the overall scale is normalized). The data show indeed the trend predicted by the MAID model. The neutron/proton cross section ratio rises significantly from the 2/3 value found earlier in the region of the $S_{11}(1535)$ resonance to higher incident photon energies. Around 1025 MeV incident photon energy, corresponding to W=1675 MeV proton and neutron cross sections are of similar size and also of similar shape. At even higher incident photon energies, the neutron cross section seems to be less forward peaked.

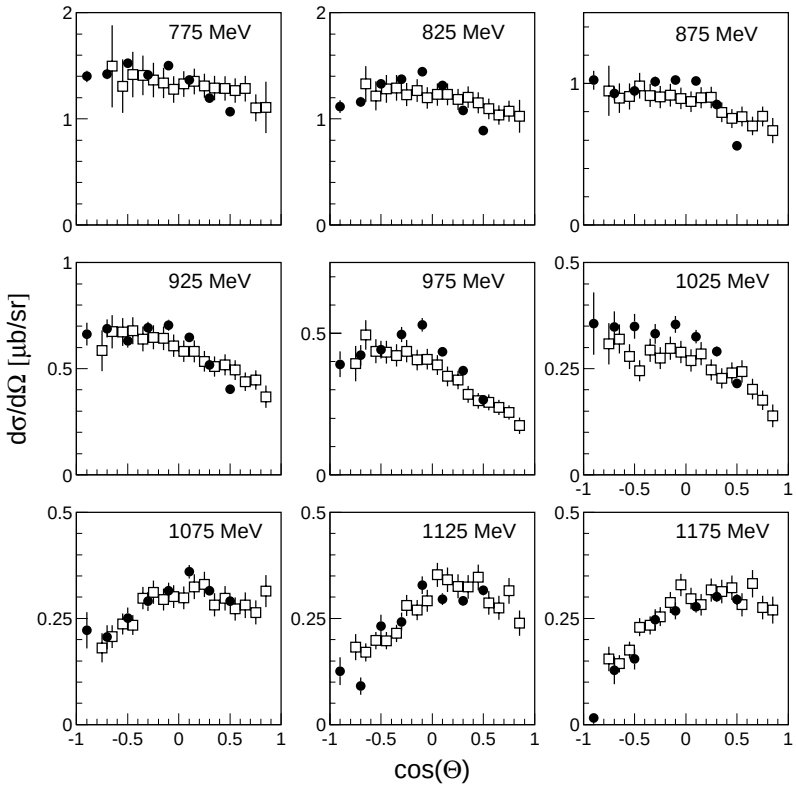

Figure 5: Angular distributions of quasifree photoproduction of η mesons from protons bound in the deuteron (filled black circles, absolute scale normalized [24]) compared to the reaction on the free proton (open squares) [16].

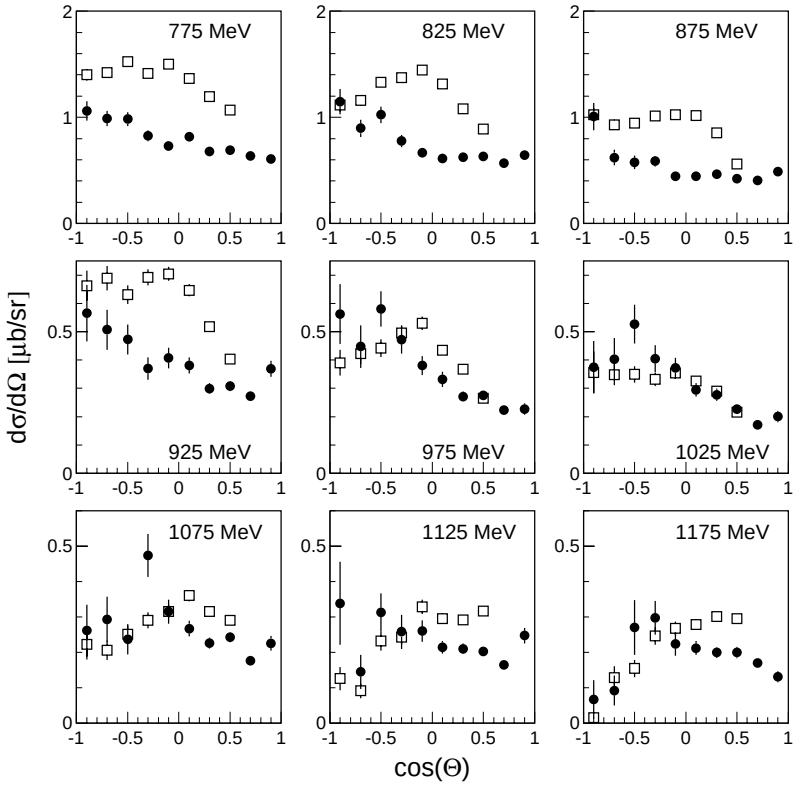

Figure 6: Angular distributions of quasifree photoproduction of η mesons from protons bound in the deuteron (open squares) compared to the quasifree reaction on the bound neutron (filled black circles, absolute scale normalized) [24]

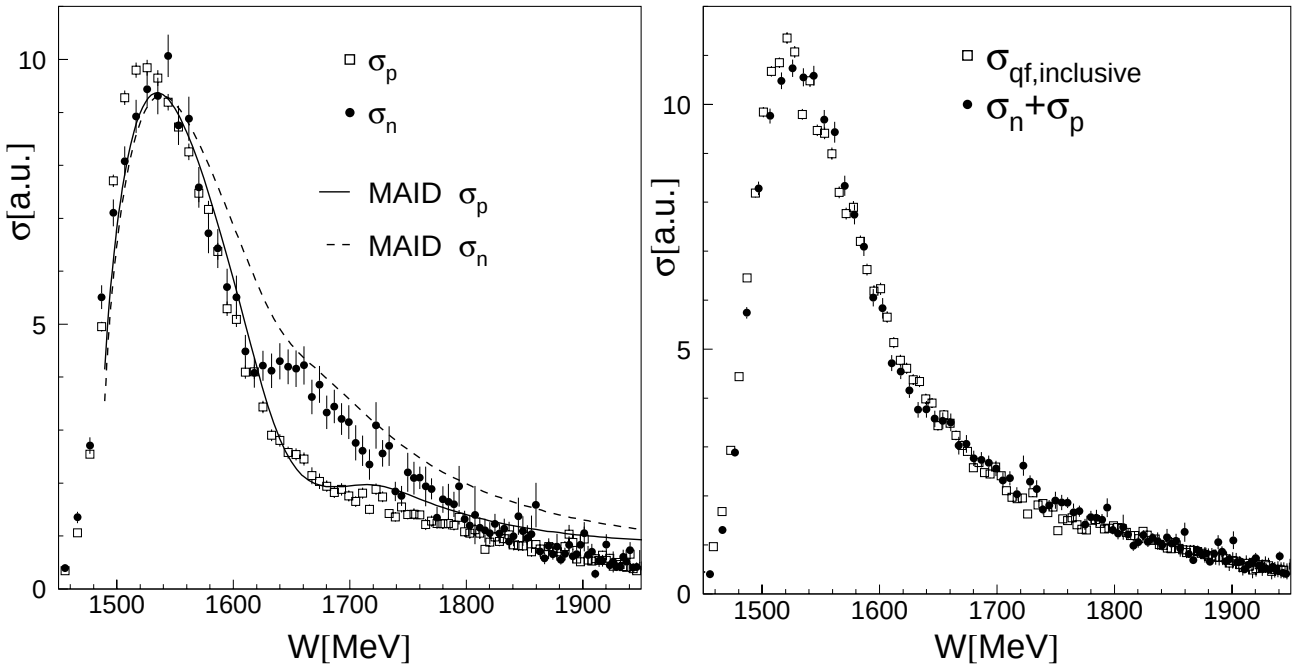

Figure 7: Left hand side: excitation functions of quasifree photoproduction of η mesons off the proton and off the neutron (both bound in the deuteron) [24]. The two curves represent the predictions of the MAID model for the two reactions [13] (absolute scales normalized in the maximum). Right hand side: excitation function for inclusive η photoproduction off the deuteron compared to the sum of the absolutely normalized exclusive proton and and neutron cross sections.

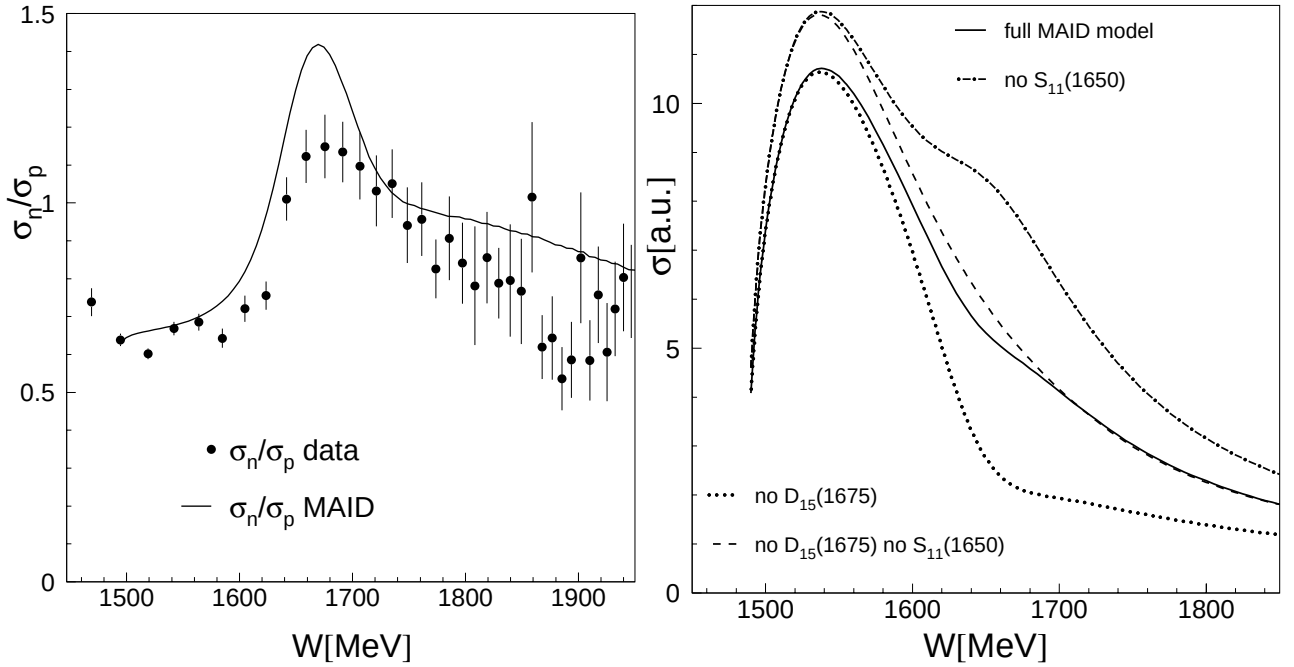

Figure 8: Left hand side: comparison of the ratio of the quasifree neutron and proton cross sections [24] compared to the prediction of the MAID model [13]. Right hand side: Predictions of the MAID model for the total neutron cross section for different resonance contributions (further resonances included in the model, apart from the strongly dominant $S_{11}(1535)$, have only negligible effects on the cross sections)

Total cross sections for the quasifree η photoproduction off the proton and off the neutron have been approximated by fits to the angular distributions. They are compared in fig. 7, left hand side. Also shown in the figure are the MAID predictions for the reaction on the free proton and free neutron. For a more easy comparison of the shape of the excitation functions, all data and model results are normalized to each other in the maximum of the first S_{11} resonance ($E_\gamma \approx 800$ MeV, $W \approx 1535$ MeV). The shape of the quasifree proton data is nicely reproduced by the MAID curve for the reaction off the free proton. The neutron data shows a bump-like structure at exactly the same energies as previously found in the GRAAL experiment. Although the MAID predictions have a similar tendency, the structure seems to be less pronounced in the model. In the right hand side of the figure the inclusive cross section (no condition on recoil proton or recoil neutron) is compared to the sum of the properly scaled (σ_n/σ_p=2/3 at W=1535) exclusive cross sections. The agreement is quite good, which is an additional check for the consistency of the data analysis.

The ratio σ_n/σ_p as function of the total cm-energy W is compared to the prediction from the MAID model in the left hand side of fig. 8. The qualitative behavior is rather similar. The right hand side of this figure summarizes the MAID predictions for different assumptions, the full model and the results when the $D_{15}(1675)$ resonance or/and the $S_{11}(1650)$ are switched off. Switching off other resonances apart from the well established, dominant $S_{11}1535$ contribution has only negligible effects. It is evident, that in the model the enhancement of the cross section around W=1675 MeV is mainly due to the excitation of the D_{15} resonance. However, a similar result can be obtained if the $S_{11}(1650)$ resonance does not contribute. This is due to a strong cancellation between the contributions from the two S_{11} resonances in this energy region. Obviously, further observables are needed to pin down the quantum numbers of the resonance which is responsible for the bump in the excitation function.

The angular distributions in this energy range are compared to the MAID predictions in the left hand side of fig. 9. For the data two different sets labeled 'unpolarized' and 'polarized' are shown. The correspond to two different beam times, one using an unpolarized photon beam, the other using a polarized beam (maximum polarization at $E_\gamma \approx 1.2$ GeV). The agreement, respectively the discrepancies between the two data sets indicate the typical systematic uncertainty of the preliminary analysis of the data. Somewhat surprisingly, the angular distribution does not at all follow the bowl shaped form predicted by MAID. This form would be typical for a significant contribution from the D_{15} as can be seen in the figure where also MAID predictions without D_{15} are shown. However, also these curves do not reproduce the data, which shows a strong enhancement at backward angles. Such a form can e.g. arise from the interference of the S_{11} with a P_{11}. Altogether, the shape of the angular distribution is not yet understood. Unfortunately, the data are much less precise in the interesting backward region. This is a simple consequence of the detection probability, which is shown in fig. 9, right hand side. The three histograms show the simulated detection probability for the η mesons in the six-photon decay channel and the combined probabilities for η mesons in coincidence with protons or neutrons. The problem is, that the η detection probability drops from almost 25 % for extreme forward angles to roughly 1 % for extreme backward angles. This is a consequence of the trigger efficiency of the Crystal Barrel/TAPS setup. Since the Barrel has no timing, only hits in TAPS or the inner detector surrounding the target can be used in the first level trigger. However, for measurements on the neutron, the inner detector is useless for trigger purposes. Furthermore, if the η goes backward, even for the six-photon decay channel the chance of having at least two photons in TAPS is small (for the same reason the two-photon decay of the η is completely useless). This is not so much a problem for measurements on proton targets, since in this case the forward going recoil proton can trigger for backward going mesons. However, this does of course not work with recoil neutrons, so that the trigger could be only constructed from photons hitting the TAPS detector. The two histograms with for the combined η - recoil nucleon detection probabilities show the expected behavior: the detection

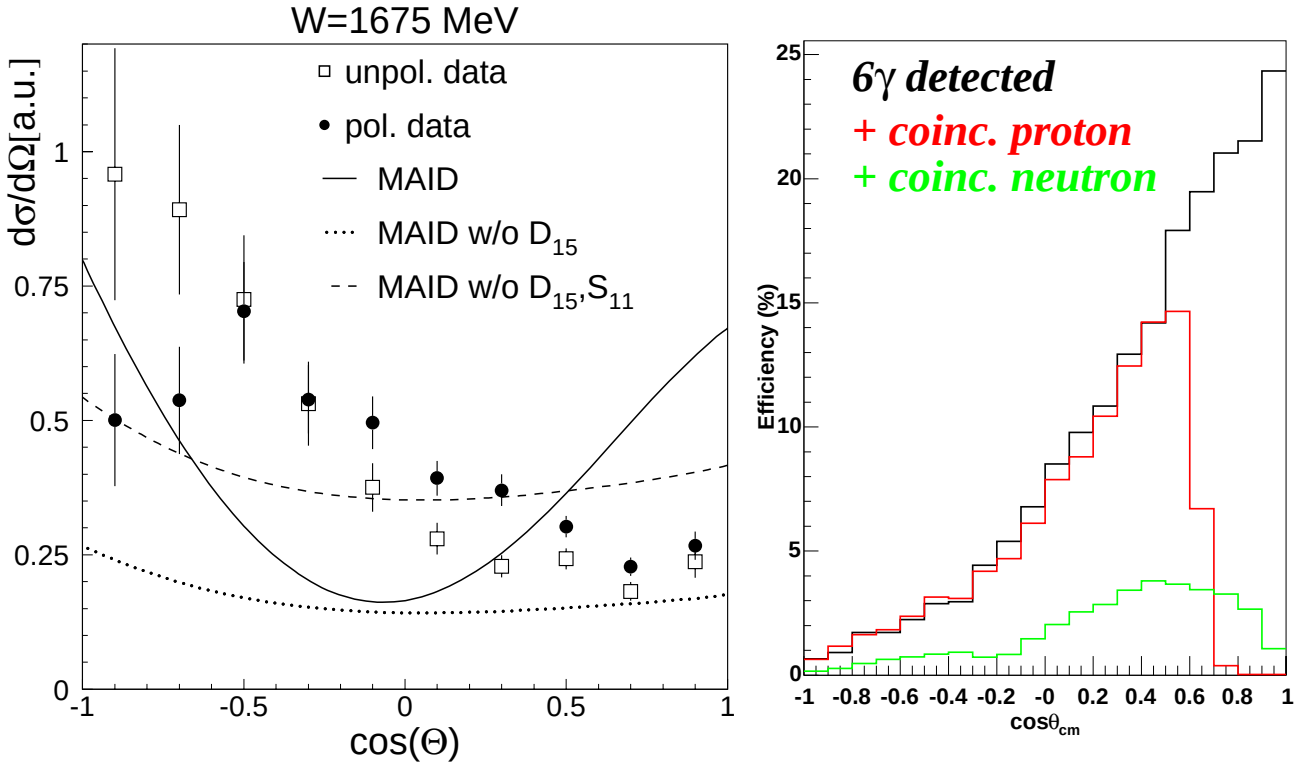

Figure 9: Left hand side: angular distribution of quasifree η photoproduction off the neutron at W=1675 MeV compared to predictions of the MAID model for different resonance contributions (S_{11} refers to the $S_{11}(1605)$). The data are preliminary results from previous the CBELSA/TAPS experiment [24]. The two data sets correspond to two different beam times using unpolarized, respectively linearly polarized photon beams. Right hand side: detection efficiency of the CBElSA/TAPS setup for η mesons ($\eta \to 3\pi^o \to 6\gamma$ decays, upper black histogram), η mesons in coincidence with recoil protons (middle red histogram), and η meson in coincidence with recoil neutron (lower green histogram) also for W=1675 MeV.

probability for protons is close to 100 % for those protons which reach the detector and drops to zero in the extreme forward range, corresponding to low-energy backward protons which are absorbed. The neutron efficiency is smaller, but always larger than zero, since there are no absorption problems.

The data taken with the linearly polarized photon beam allow the extraction of the photon beam asymmetry Σ. Two different settings were measured, one with the maximum polarization at 1.2 GeV photon energy (corresponding to W=1.77 GeV) and one with the maximum at 1.6 GeV (W=1.97 GeV). The preliminary results at Θ=90^o are summarized in fig. 10. The left hand side of the figure shows the asymmetry for the quasifree proton. They are compared to the MAID prediction for the free proton with and without excitation of the D_{15}. Both model results are very similar in the proton case, and the data seem to follow the same trend. In the neutron case (right hand side of the figure) the predictions with and without D_{15} resonance are quite different. In contrast to the angular distributions, the asymmetries seem to be in better agreement with the calculation including he D_{15} resonance. Unfortunately, in particular the data with the higher polarization peak setting are only of very limited statistical quality.

In summary, the measured quasifree proton data are in quite reasonable agreement with previous results from the free proton, giving support to the assumption that the quasifree measurements off the deuteron can be straight forward interpreted as good approximation of the free nucleon case. The quasifree neutron data show a bump-like structure at the same energy as

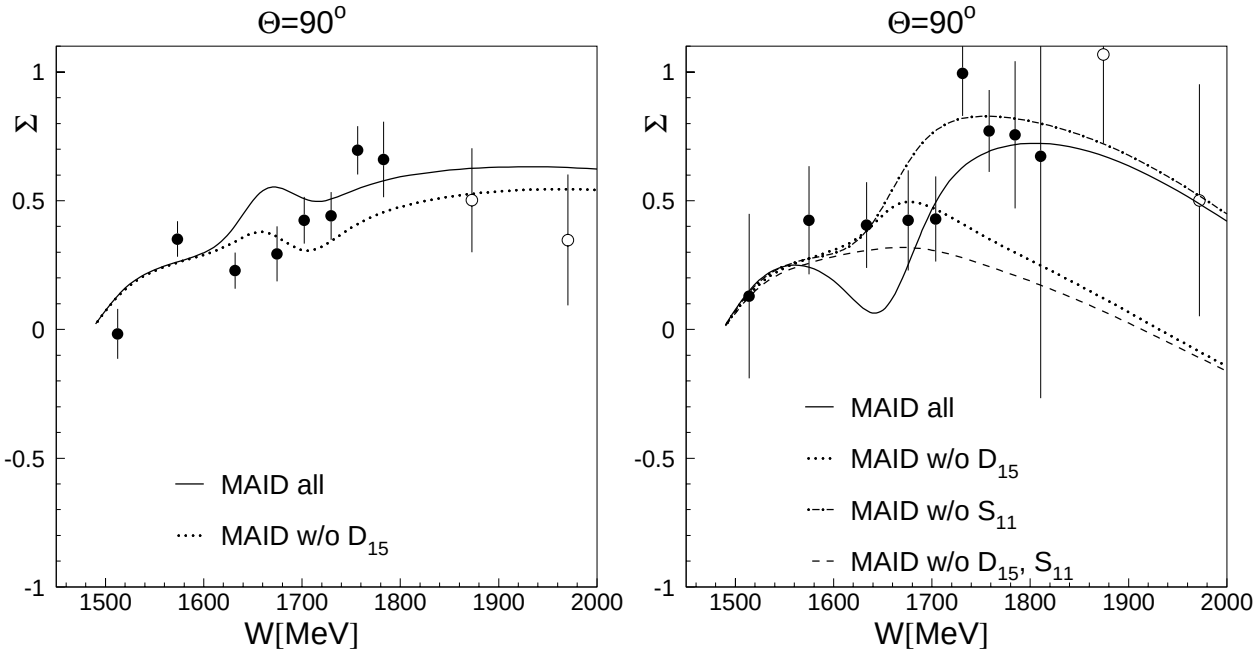

Figure 10: Left hand side: Photon beam asymmetry as function of W for Θ=90^o for quasifree η photoproduction from the bound proton [24] compared to predictions of the MAID model [13]. Right hand side: same for quasifree photoproduction off the neutron (S_{11} refers to $_{11}(1650)$. Data are for a $\pm 30^o$ range. Full (open) points: polarization peak at 1.2 (1.6) GeV.

previously reported from the GRAAL experiment. The preliminary photon beam asymmetries are in reasonable agreement with a version of the MAID model which explains the enhancement of the neutron cross section with respect to the proton case by a contribution of the $D_{15}(1675)$ resonance, but the angular distributions show a different behavior.

1.3 Predicted sensitivity of different observables

We have already discussed the sensitivity of angular distributions and photon beam asymmetry to different resonance contributions in the previous section. However, the sensitivity of double polarization observables is even larger. The two observables of special interest are the 'GDH-observable' E (circularly polarized photon beam on longitudinally polarized target) and the observable G (linearly polarized photon beam on longitudinally polarized target). The energy dependence of these two observables at Θ=90^o predicted by MAID for different resonance contributions is shown in fig. 11. Both observables have a very large sensitivity to the $D_{15}(1675)$ resonance. E will stay close to unity over the whole energy range if the D_{15} does not contribute. If on the other hand it contributes, E will sharply drop from +90 % to -50 % (as long as we take the contribution of the second S_{11} for granted, but even without it would drop from +90 % to +10 %). For the G observable a strong peak approaching almost unity is predicted in presence of the D_{15}, while in its absence G would slowly and smoothly rise from zero to $\approx$+30 %. The nice thing is, that not only the sensitivity of this two observables is large, but in all scenarios with and without D_{15} at least for one observable also the absolute values will be large (actually close to unity). The E observable should also allow to distinguish between the scenario with D_{15} and $S_{11}(1675)$ and the (improbable) D_{15} without $S_{11}(1675)$ scenario.
The measurement of the unpolarized cross sectionσ_o and of E allows also to extract the helicity 1/2 and 3/2 cross sections via

$$\begin{aligned} \sigma_{1/2} &= \sigma_o(1+E) \\ \sigma_{3/2} &= \sigma_o(1-E) \ . \end{aligned} \tag{5}$$

Predictions for the two helicity components are shown in fig. 11, bottom . The D_{15} resonance would in particular produce an unambiguous signal in the helicity 3/2 component. Actually already the measurement of the total helicity 1/2 and 3/2 cross sections would allow to establish or rule out the contribution of the D_{15}. The helicity 1/2 component is of course sensitive to the contribution of the second S_{11} , which can not contribute to the 3/2 channel.

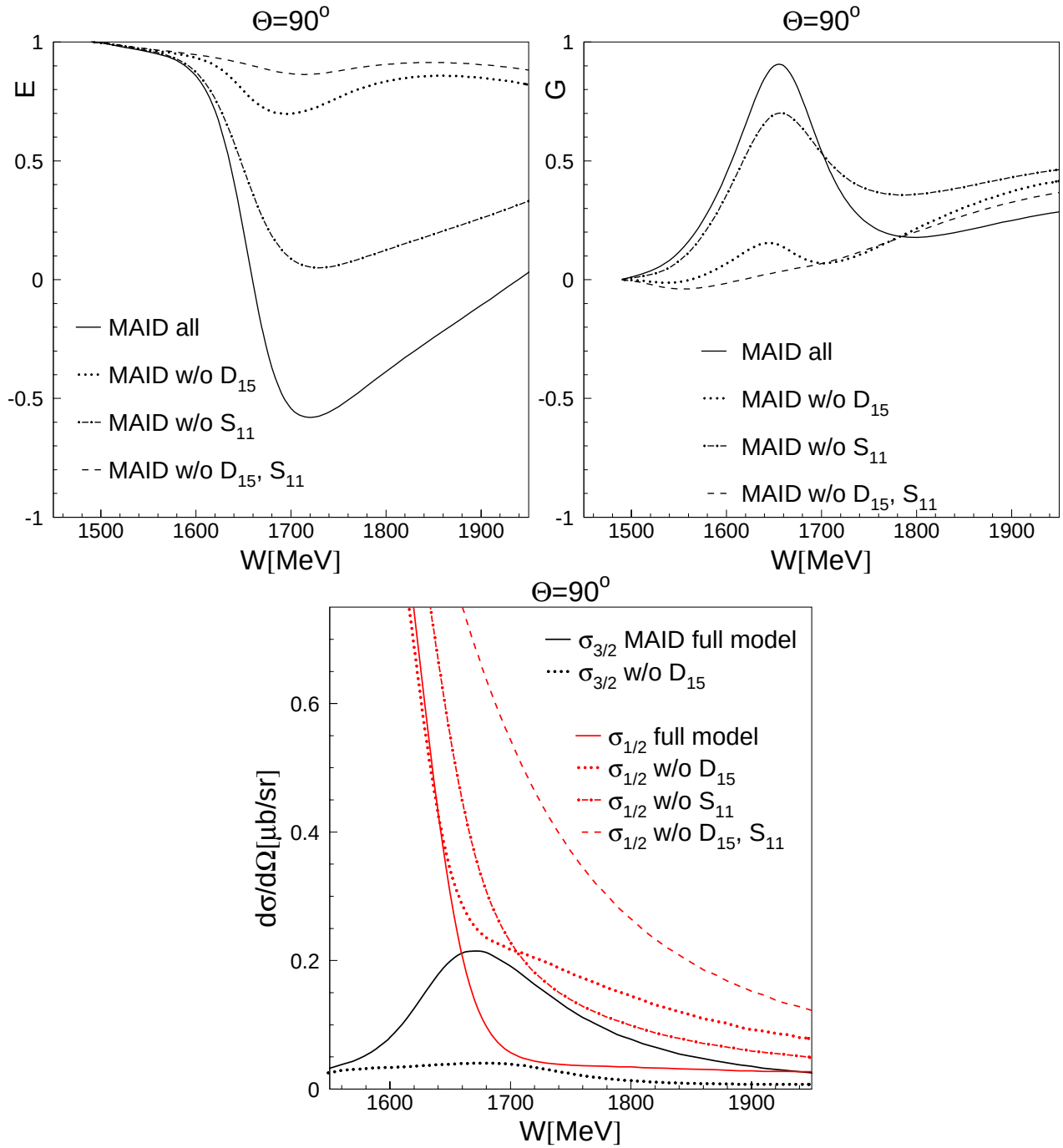

Figure 11: Upper part: Sensitivity of the double polarization observables E and G at Θ=90^o as function of W to resonance contributions in the MAID model [13]. lower part: Sensitivity of the $\sigma_{3/2}$ and $\sigma_{1/2}$ contributions in the MAID model [13] to the $D_{13}(1675)$ and $S_{11}(1670)$ resonances.

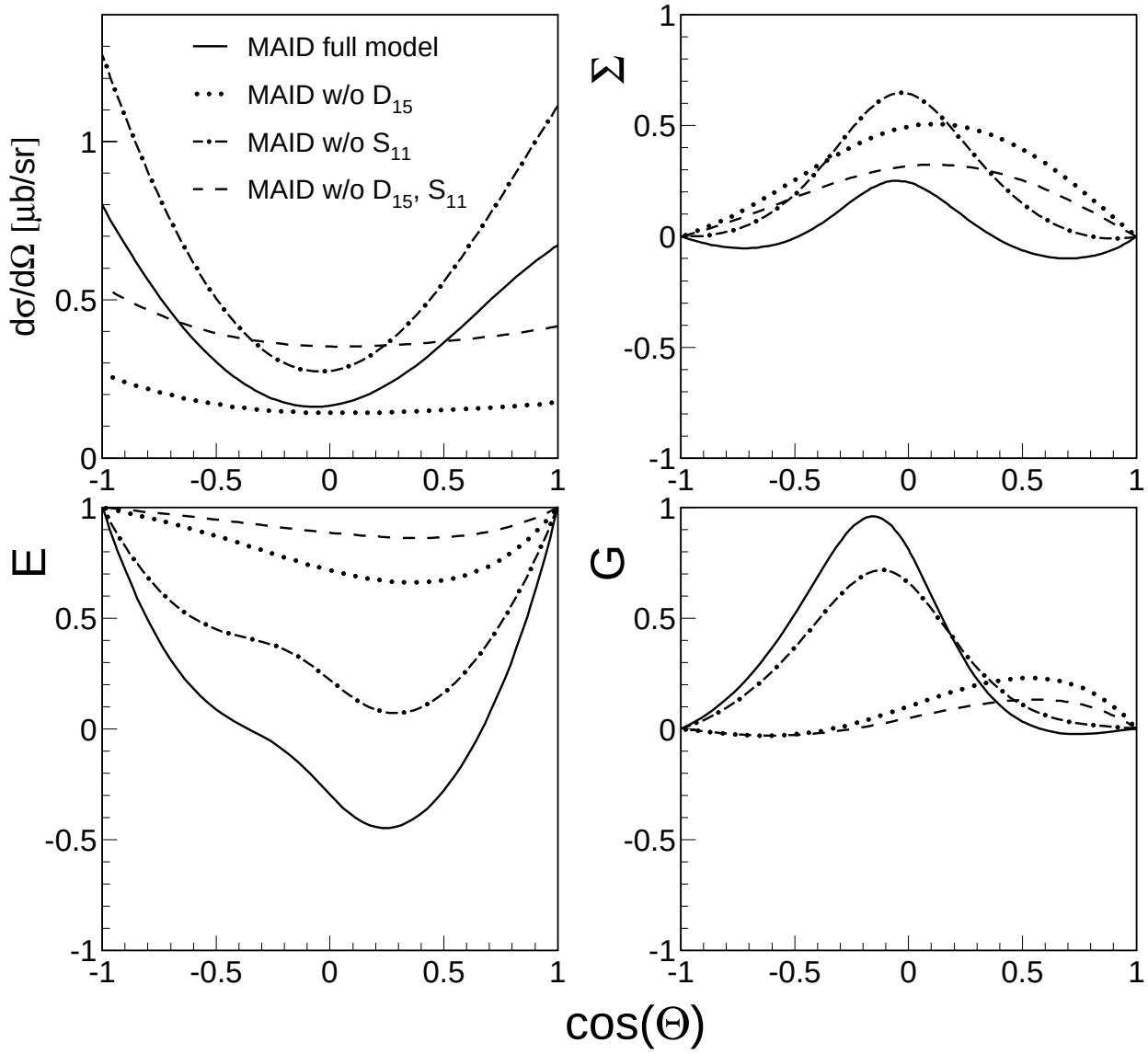

Figure 12: Sensitivity of the angular distributions, photon beam asymmetry and the double polarization observables E and G as function of cos(Θ) at W=1675 MeV to resonance contributions in the MAID model [13].

The predicted angular distributions of all discussed observables in the maximum of the resonance bump at W=1675 MeV are summarized in fig. 12. They underline again the large sensitivity of the double polarization observables. Measurements of this set of four observables should allow an almost unambiguous extraction of the resonance contributions. We therefore propose to re-measure the angular distributions and the photon beam asymmetry Σ with higher statistical accuracy and to do a first measurement of the two double polarization observables. As a final remark one should mention, that in general predictions for the sensitivity of observables require re-fits of the model since simply switching off resonances can produce unreliable results due to interferences between them. However, due to the non-availability of neutron data, the MAID model was only fitted to the proton and the neutron cross sections were predicted using known coupling constants. Furthermore, the D_{15} is so dominant in the $\sigma_{3/2}$ component (there are no other resonance with significant contributions to this channel in the model), that its influence on the observables is only little dependent on the contributions of other resonances. Even the impact of the second S_{11} is probably overestimated, since its elimination would have an impact on the parameters of the first S_{11}, which would at least partly compensate the effect.

2 Photoproduction of η' mesons from the deuteron at threshold

Our previous letter of intent (ELSA/2-2003) about η' photoproduction off the nucleon [25] aimed at the detailed investigation of resonance contributions to η' photoproduction and at the study of the η' -nucleon interaction. Since the second aspect requires the measurement of η' photoproduction from the deuteron in the immediate threshold region, it can be better done at MAMI C. In fact, the data can be taken simultaneously with the η production measurement. Therefore we include this aspect here.

The interaction of mesons with nucleons and nuclei is one of the central issues in strong interaction physics. Detailed experimental and theoretical studies of the pion - nucleon and pion - nucleus interaction have largely contributed to this field. However, much less is known in case of the heavier pseudoscalar mesons, the η- and η'-mesons, which due to their short lifetimes are not available as beams. At small meson - nucleon relative momenta the situation for η-mesons, and η' mesons at one side and pions at the other side is very different. This is due to the fact that in contrast to pions, η and η' mesons seem to couple strongly to resonances in the threshold region. In the case of η production it is well known that the reaction in the threshold region is dominated by the excitation of the $S_{11}(1535)$. In case of the η' the contribution from different resonances have not yet been identified clearly, however, the energy and angular dependencies of the cross section also suggest strong contributions from nucleon resonances.

During the last few years, we have studied in detail the photoproduction of η mesons from light nuclei (^{2}H, ^{3}He, ^{4}He) at threshold [4, 6, 8, 9, 10]. For all nuclei a significant threshold enhancement over the predictions from the impulse approximation was found. In the meantime

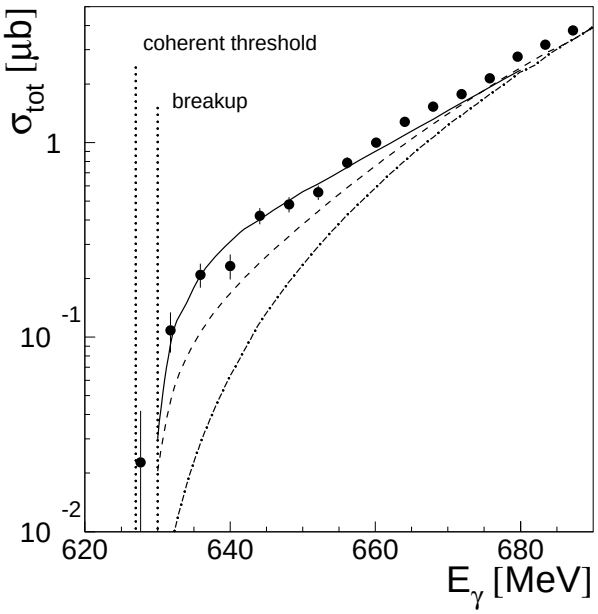

Figure 13: Inclusive η photoproduction cross section from the deuteron. The three calculations [28, 29] correspond to the impulse approximation (dash-dotted), IA plus NN-FSI (dashed), and IA plus NN- and ηN-FSI (solid).

in the deuteron case model calculations from different groups became available which explain most of the enhancement via NN and $N\eta$ FSI effects. Ritz and Arenhövel have extended their earlier work on η-photoproduction from the deuteron [26] to a Faddeev type three-body calculation of the $NN\eta$-system [27] with separable two-body interactions. In this calculation they find that the ηNN three-body aspects are important in the threshold region. Sibirtsev

and coworkers have studied in detail the influence of NN and ηN final state interaction (FSI) on the threshold behavior [28, 29]. Their result is compared to the data in fig. 13.
Final state interaction is obviously not important at excess energies above the threshold of more than ≈50MeV where the data agree with the impulse approximation. Close to threshold NN FSI plays an important role. Although ηN FSI alone does not give rise to a strong enhancement of the cross section, Sibirtsev et al. find that a constructive interference between NN and ηN FSI is important. The result of the complete model calculation reproduces the data quite well. This finding is somehow in line with the results from Fix and Arenhövel [27], who also found that NN FSI alone cannot reproduce the data but three-body effects of the $NN\eta$-system must be accounted for. The comparison of such model calculations to the threshold data offers one of the few possibilities to study the meson-nucleon interaction. In the case of η photoproduction this line of research has finally led to the search for η - nucleus bound states (so-called η-mesic nuclei).
In the case of η' mesons much less is known about the meson-nucleon interaction. In the proposed experiment we will make a first study of the threshold behavior of η' production on the deuteron and search for possible enhancement effects. This experiment can be done together with the measurement of the angular distributions of η production and will thus not require additional beam time. The energy range of interest is between E_γ=1200 MeV (threshold for coherent production on the deuteron) and E_γ=1450 MeV (threshold on the free nucleon) and thus well suited for MAMI C.

3 Proposed experiments

3.1 General considerations

We propose to measure the angular distributions and the double polarization observable E with the Crystal Ball/TAPS setup at MAMI C and the photon beam asymmetry Σ and the double polarization observable G with the Crystal Barrel/TAPS setup at the ELSA accelerator. This suggestion is based on the following considerations.
The proposed experiments require the following beam/target combinations:

- $d\sigma/d\omega$: unpolarized liquid deuterium target, unpolarized (or circularly polarized) photon beam
- Σ: unpolarized liquid deuterium target, linearly polarized photon beam (polarization maxima between 800 - 1600 MeV beam energy)
- E: longitudinally polarized deuterium target, circularly polarized photon beam
- G: longitudinally polarized deuterium target, linearly polarized photon beam

Both target types will be available at MAMI as well as at ELSA. The two measurements which require the linearly polarized photon at energies above 1 GeV (Σ, G) must be done at ELSA since reasonable polarization degrees in this energy will not be available at MAMI C. The measurements with the unpolarized beam, respectively the circularly polarized beam could be done in principal in Mainz or in Bonn. However, in this case it is clearly advantageous to do the measurements in Mainz. One point is, that the achievable beam intensities are higher. However, more important is, that the detector setup in Mainz is much better suited for this type of experiments. Since the Crystal Ball has timing information, in contrast to the Barrel it can be used in the first level trigger. This means that for the six-photon decay channel of the η meson the detection efficiency will not significantly drop to backward angles as in case of the barrel (see fig. 9, so that we win roughly an order of magnitude in detection efficiency at backward angles. For the same reason, we can also use the two-photon decay of the η meson. This will not only lead to another gain of more than a factor of two in counting statistics. It will also allow better checks of systematic effects in the detection efficiency.
Both experiments require the use of almost 4π electromagnetic calorimeters. Apart from the Crystal Ball in Mainz and the Crystal Barrel in Bonn, the TAPS detector will be in the forward region. Originally, I had been planned to operate TAPS together with the Crystal Ball in Mainz until 2007 and move it to Bonn in 2008. However, this schedule would have resulted in severe restrictions for the experimental program in Bonn (late start) and in Mainz (stop before the double polarization program could be run). The TAPS, Crystal Ball and Crystal Barrel collaborations have therefore agreed on a different scenario, which allows parallel running at MAMI C and ELSA with only a very minor performance loss. The forward wall in Mainz will be reduced by the two outer rings of BaF_2 modules. This modified forward wall consisting of 384 modules can still cover the forward range in Mainz when moved closer to the Ball. This is possible without serious mechanical problems and the target - TAPS distance will be still larger than one meter. The modification will be finished during the time window for the tagger upgrade. The removed crystals, some additionally available modules, together with 30 crystals, which will be newly bought are sufficient to construct a second forward wall of 216 modules. This setup, together with the forward plug developed for the Crystal Barrel will cover the need of the Bonn setup. The implications are, that both experiments can run in parallel in 2006 - 2008, at the price of a very modest reduction in angular and time-of-flight reduction. The additionally necessary hardware (crystals, photomultiplier, read-out electronics) are financed by the Basel, Bonn and Giessen groups.

3.2 Measurements with Crystal Ball/TAPS at MAMI C

The MAMI C part of the experiment requires two separate measurements

- Measurement I: angular distributions for η production off the quasifree neutron
- Measurement II: double polarization observable E (circularly polarized photon beam on longitudinally polarized target) off the quasifree neutron

which require the following beam, target and detector hardware.

3.2.1 Photon beams

Both measurements can run with circularly polarized photon beams with the highest energy available at MAMI C (presumably 1.5 GeV). Measurement I) could as well run with an unpolarized beam (circular polarization for a two-body final state without target polarization gives of course no additional information). However, with a circularly polarized beam, the same beam time could be used for an exploratory study of the circular polarization observable in the three-body final state reaction $\gamma n \to n\eta\gamma'$ (see proposal: Magnetic moment of the $S_{11}(1535)$). The circularly polarized photon beam is essential for the measured of E. The typical energy

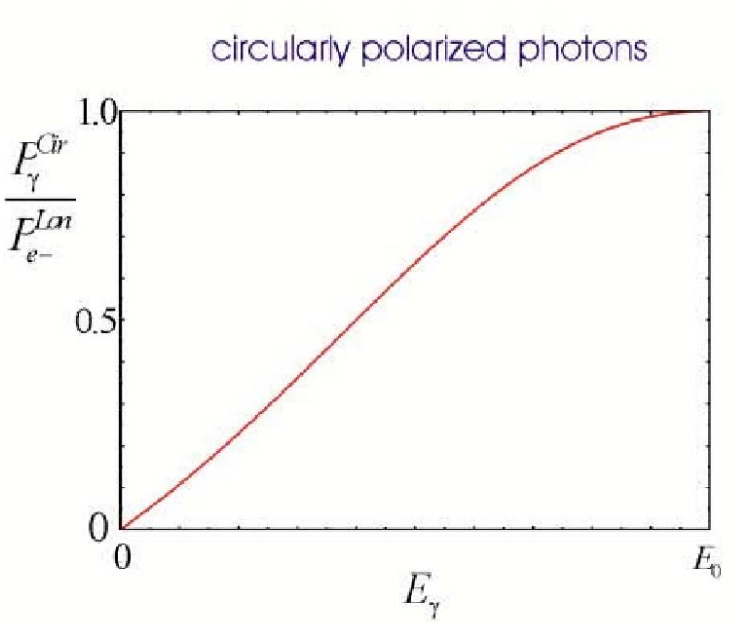

Figure 14: Polarization transfer from longitudinally polarized electrons to circularly polarized photons.

dependence of the polarization degree is shown in fig. 14. The polarization transfer from the longitudinally polarized electrons to circularly polarized photons is unity at the endpoint and vanishes for small photon energies. The electron source (strained GaAs crystals) at MAMI delivers routinely electrons with polarization degrees around 75 %, so that photon polarization degrees between 0.45 and 0.75 are achieved in the energy region between $E_\gamma = E_o/2$ and $E_\gamma \approx E_o$ (E_o electron beam energy).
For this proposal, we will run with the maximum incident photon energy of 1.5 GeV, so that polarization degrees above 0.45 will be available above 750 MeV incident photon energy (corresponding to W=1500 MeV). This means that the range of interest can be covered with one beam setting, and in the most interesting region around 1 GeV photon energy polarization degrees around 0.5 will be reached.

3.2.2 Targets

The measurement of the angular distributions will be done with the standard liquid deuterium target of 5 cm length (corresponding to N_d=0.26 b^{-1}).
The E measurement will use a frozen-spin deuterated butanol (C_4D_9OD) target. Which is currently under construction in Dubna. A very similar target was already successfully used in the GDH experiment in Mainz and in Bonn. Fig. 15 shows the time development of the

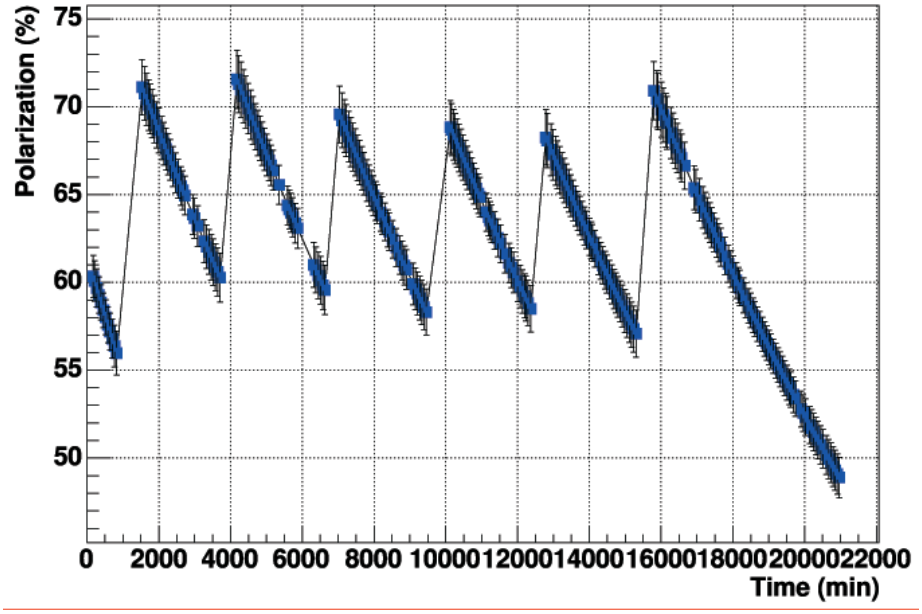

Figure 15: Time evolution of the polarization degree of a deuterated butanol target during the Mainz GDH measurement over a two weeks period [30].

measured target polarization degree [30]. Recently, with a new doping technique it became possible to reach polarization values above 70 % with relaxation times above 100 hours. This means that longtime averages of the polarization degree on the order of 0.6 can be reached.
The polarization is diluted by the unpolarized neutrons from the carbon and oxygen nuclei. By simply counting the number of polarized and unpolarized neutrons a dilution factor of

$$f_o = \frac{10}{42} = 0.24 \tag{6}$$

is obtained. This is however to pessimistic, first the cross sections off nuclei do not scale with the mass number (due to FSI effects), secondly a significant part of the unpolarized background can be removed with cuts on the reaction kinematics ('missing mass') since due to Fermi motion and final state interaction this spectra are more broadened for the photoproduction off C, O compared to the deuteron. Typical missing mass spectra for η production from the deuteron and from carbon at an incident photon energy of 1 GeV measured with the Crystal Barrel and TAPS at ELSA in coincidence with recoil neutrons are shown in fig. 16. The effective dilution factor can be determined by a comparison of these spectra. It is estimated by:

$$f_{eff} = \frac{10 \cdot N_d}{10 \cdot N_d + 16/3 \cdot N_C} \tag{7}$$

where N_d, N_C are the counts normalized to the photon flux and number of target nuclei in the window around zero that will be used for the analysis. Due to the chemical composition of butanol deuterium enters with a weight of 10. Carbon enters with a weight of 4, and oxygen is scaled as 8/6 of carbon, so that the unpolarized neutrons contribute with 16/3 of the carbon

cross section. The effective dilution factors calculated this way range between 0.8 and 0.5 for incident photon energies from 0.7 to 1.5 GeV.) on average we assume f_{eff}=0.7. We assume the same reduction factor for the background from the target windows, which without cuts contributed C=4 in the GDH experiments. This corresponds relative backgound contributions of to the count rates of $B = 1/f - 1$=0.43 for the butanol and C=0.54 for the target cell. With this the total dilution of the asymmetry is estimated as:

$$\eta = 1 + B + C \approx 2 \quad . \tag{8}$$

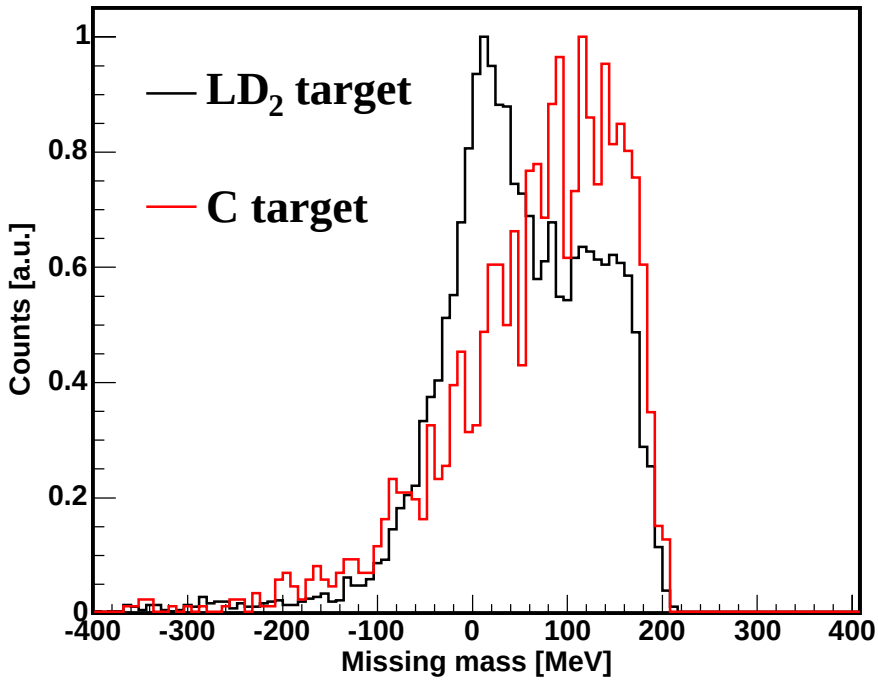

Figure 16: Missing mass spectra for the reaction $\gamma n \to n\eta$ for a deuteron and a carbon target at 1 GeV incident photon energy (arbitrary units)

3.2.3 Detector setup

The detection of the η mesons and coincident recoil nucleons will be done with the Crystal Ball and TAPS detectors as shown in fig. 17 The η mesons will be identified in the $\eta \rightarrow 2\gamma$ and the

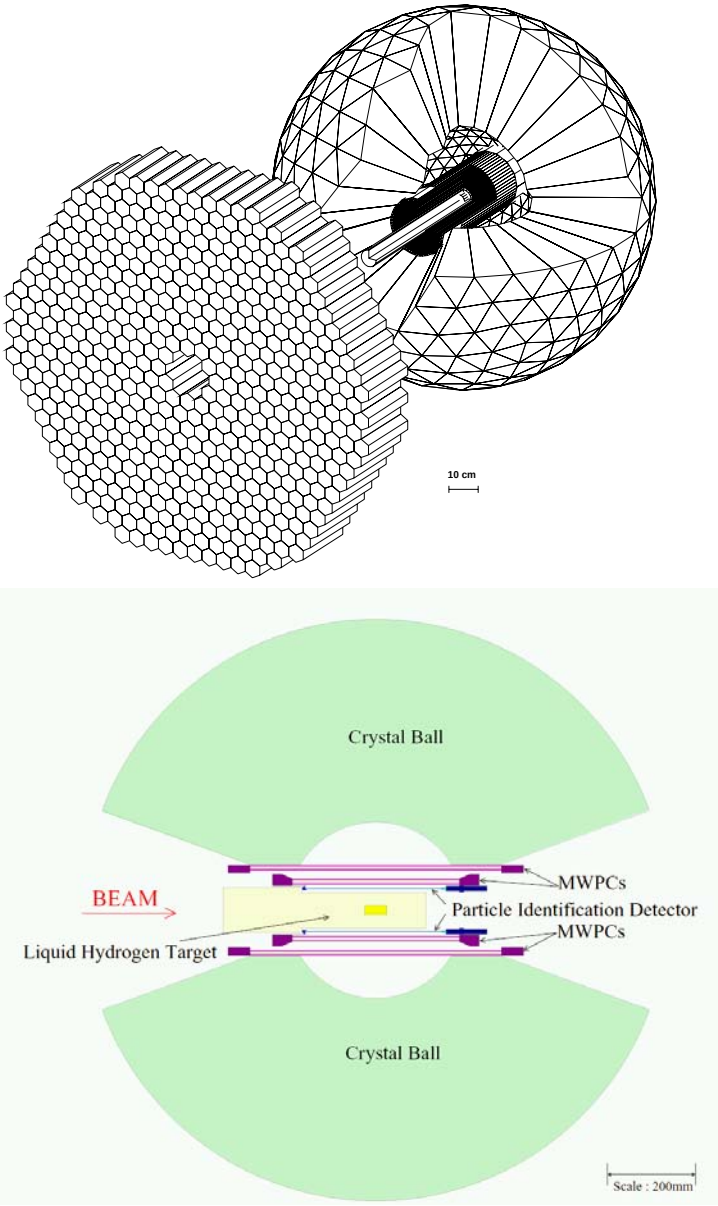

Figure 17: Upper part: combined Crystal Ball - TAPS setup as used for the previous experiments. For the proposed experiment TAPS will be reduced to 384 modules. Lower part: side view of the Ball with inner detectors.

$\eta \rightarrow 3\pi^o \rightarrow 6\gamma$ decay channels by detection of the decay photons in the calorimeter and the application of standard invariant and missing mass techniques as in previous experiments.
The recoil nucleons will be also detected in the calorimeters and identified with the help of charged particle veto detectors (TAPS), particle identification detectors and wire chambers (Ball) and time-of-flight versus energy techniques. Measured detection efficiencies for recoil neutrons in TAPS and the Ball are summarized in fig. 18.
Detection efficiencies have been simulated based on the analysis done for the previous data form Crystal Barrel/TAPS. They are summarized in fig 19. These simulations take into account all cuts used for the clean identification of the quasi-free reactions, also cuts on time-of-flight versus energy etc. for the identification of recoil nucleons.

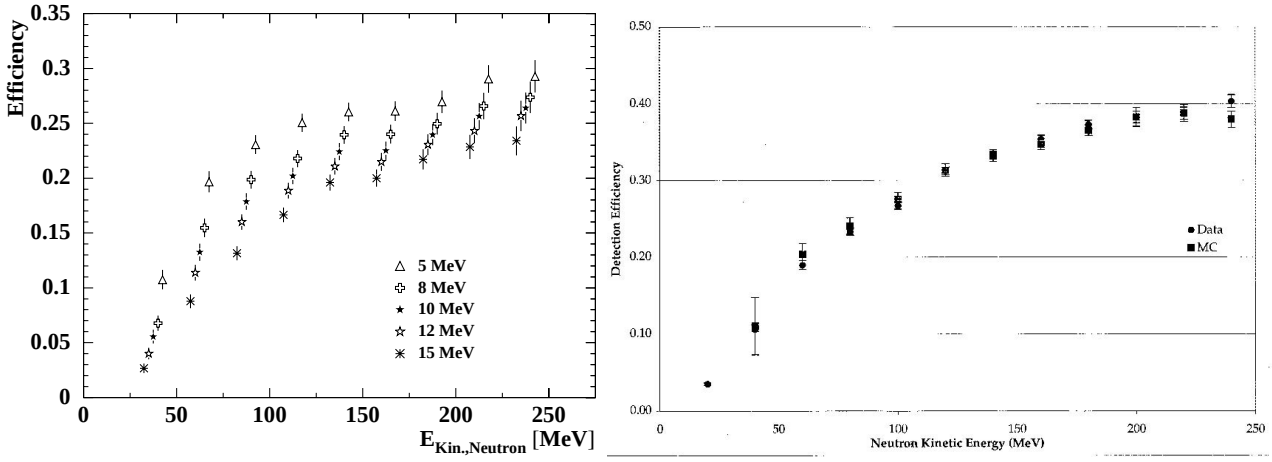

Figure 18: Measured neutron detection efficiencies for TAPS (left hand side, for different detector thresholds) and the Crystal Ball (right hand side)

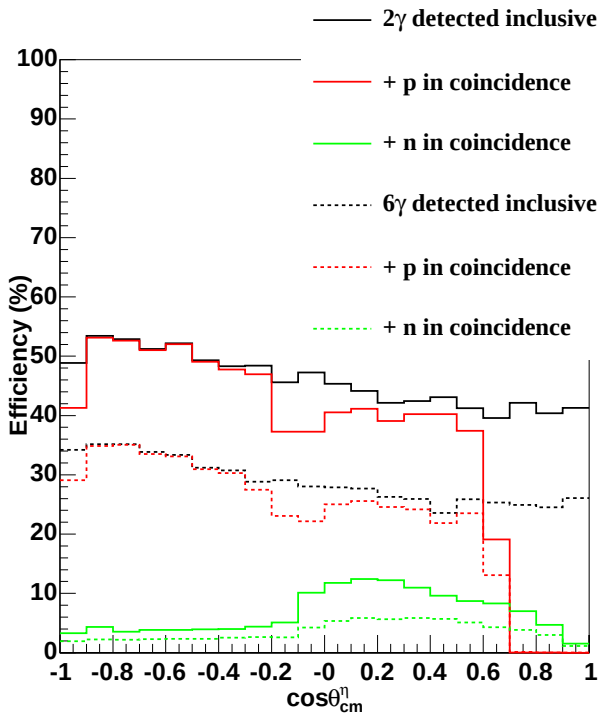

Figure 19: Simulated detection efficiencies for the coincident detection of η-mesons and recoil nucleons

3.3 beam time estimates

For the measurement of the angular distributions we aim at a statistical precision of 10 % for angular distributions in 10 bins of $\cos(\Theta)$ and roughly a 20 MeV binning of incident photon energies. The necessary beam time is given by

$$\Delta t = [\delta^2_{stat} \cdot \Delta\sigma_o \cdot N_\gamma \cdot N_t \cdot \epsilon \cdot b]^{-1} \tag{9}$$

with the following notation:

- δ_{stat}: relative statistical uncertainty $\Rightarrow$ **0.1**
- N_γ: number of photons per 10 MeV incident photon energy $\Rightarrow$ **1.75**$\cdot$ **10**^{5}**sec**$^{-1}$
- N_t: surface density of target nuclei (5 cm liquid deuterium target) $\Rightarrow$ **0.25 b**$^{-1}$
- ϵ: detection efficiency, assumed on average as $\Rightarrow$ **0.05**
- b: decay branching ration of η mesons, for $\eta \to 2\gamma \Rightarrow$ **0.4**
- $\Delta\sigma_o$: unpolarized cross section in the respective angular bins.
  We assume $d\sigma/d\Omega \approx 0.2$ μb/sr, corresponding to $\Rightarrow$ $\Delta\sigma_o$**=0.16** μ**b** at $\cos(\Theta)$=$\pm$0.9

With these numbers we arrive at a beam time estimate of

200 hours

For the measurement of the double polarization observable E we will increase the energy binning to 40 MeV incident photon energy (corresponding to roughly 20 MeV in W) and require a statistical uncertainty for E of δE_{stat}=0.15 for a minimum cross section of $\Delta\sigma_o$=0.3μb.
The necessary beam time can be calculated from

$$\Delta t = \eta[P^2 \delta E^2_{stat} \cdot N_\gamma \cdot N_T \cdot \epsilon \cdot b \cdot \Delta\sigma_o]^{-1} \tag{10}$$

with the following notation:

- ΔE_{stat}: statistical uncertainty of $E \Rightarrow$ **0.15**
- N_γ: number of photons per 40 MeV incident photon energy $\Rightarrow$ **7**$\cdot$ **10**^{5}**sec**$^{-1}$
- N_t: surface density of target nuclei (2 cm frozen butanol target) $\Rightarrow$ **0.09 b**$^{-1}$
- ϵ: detection efficiency, assumed on average as $\Rightarrow$ **0.05**
- b: decay branching ratio of η mesons, for $\eta \to 2\gamma \Rightarrow$ **0.4**
- $\Delta\sigma_o$: unpolarized cross section in the respective angular bins.
  We assume minimal $\Rightarrow$ $\Delta\sigma_o$**=0.3** μ**b**
- P: product of polarization degrees $\Rightarrow$ $P_t \cdot P_b$**= 0.6**$\times$**0.5=0.3**
- $\eta = 1 + B + C$ effective dilution from unpolarized background $\Rightarrow$ **2.0**

With these numbers we arrive at a beam time estimate of

700 hours

The expected quality of the data under this assumptions is shown in fig. 20. Shown are simulated results for the angular distribution (200 h beam time) and the polarization observable E (700 h beam time). The cross sections, respectively asymmetries are taken from MAID for the scenarios with and without D_{15}. For this calculations proper energy and angular dependencies of cross sections, efficiencies and polarization degrees have been taken into account.

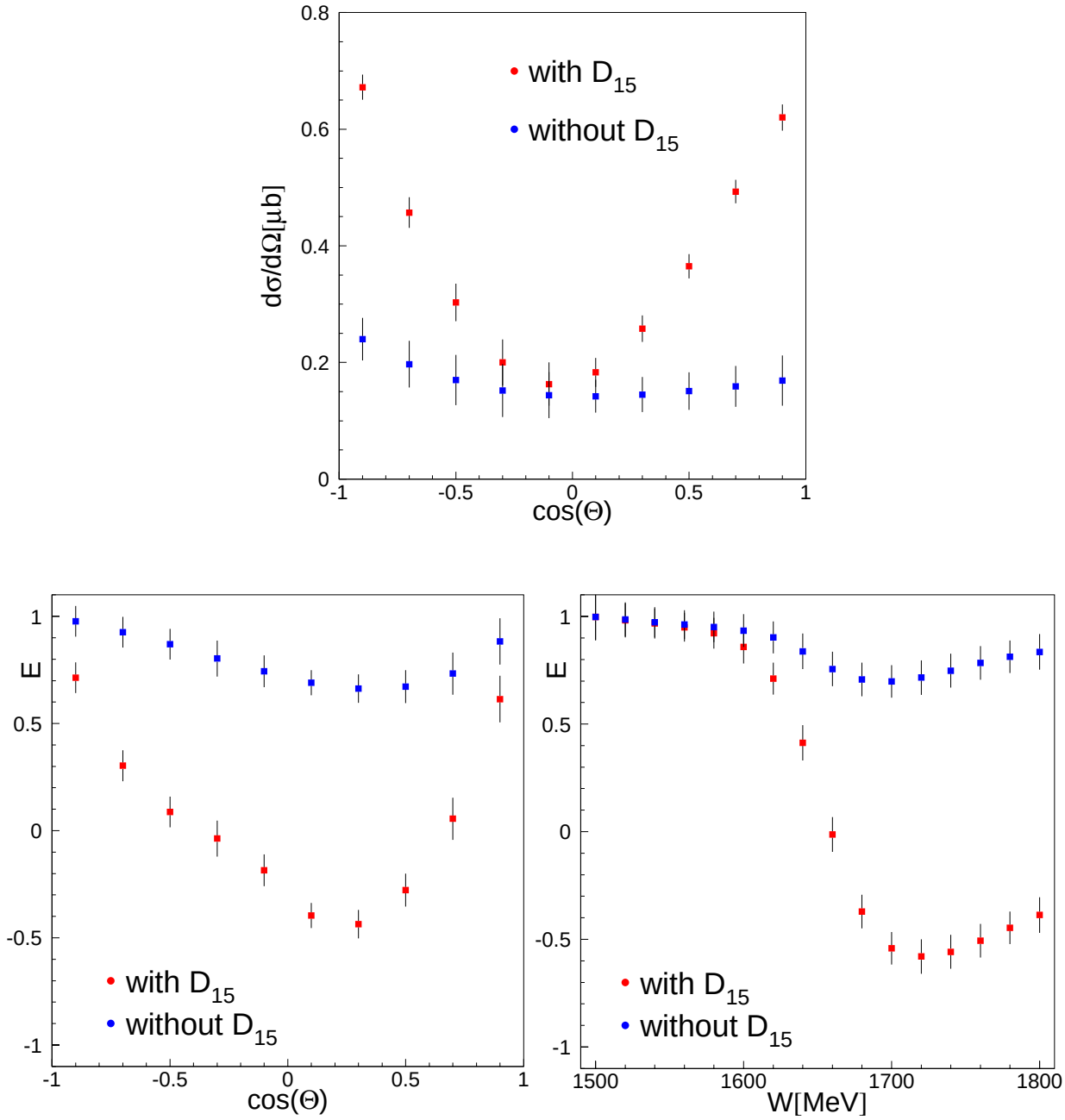

Figure 20: Upper part: simulated statistical accuracy for the angular distribution at W=1675 MeV. Lower part: statistical accuracy for the double polarization observable E, left hand side: as function of cosΘ at W=1675 MeV, right hand side: as function of W for Θ=90^o (Θ between 80^o und 100^o). The two data sets correspond to the MAID predictions with and without D_{15} resonance

References

[1] B. Krusche et al., Eur. Phys. J. **A6** (1999) 309

[2] E.M. Darwish, H. Arenhövel, M. Schwamb, Eur. Phys. J. **A16** (2003) 111

[3] B. Krusche and S. Schadmand, Prog. Part. Nucl. Phys. **51** (2003) 399

[4] B. Krusche et al., Phys. Lett. **B358** (1995) 40

[5] P. Hoffmann-Rothe et al., Phys. Rev. Lett. **78** (1997) 4697

[6] V. Hejny et al., Eur. Phys. J. **A6** (1999) 83

[7] J. Weiss et al., Eur. Phys. J. **A11** (2001) 371

[8] V. Hejny et al., Eur. Phys. J. **A13** (2002) 493

[9] J. Weiss et al., Eur. Phys. J. **A16** (2003) 275

[10] M. Pfeiffer et al., Phys. Rev. Lett. **92** (2004) 252001

[11] N. Kaiser, P.B. Siegel, W. Weise, Phys.Lett. **B362** (1995) 23

[12] N. Kaiser, T. Waas, W. Weise, Nucl. Phys. **A612** (1997) 297

[13] W.-T. Chiang, S.N. Yang, L. Tiator, D. Drechsel, Nucl. Phys. **A700** (2002) 429

[14] S. Eidelmann et al., Phys. Lett. B 592 (2004) 1

[15] V. Burkert et al., Phys. Rev. **C67** (2003) 035205

[16] V. Crede et al., Phys. Rev. Lett. **94** (2005) 012004

[17] R.A. Arndt, Ya.I. Azimov, M. Polyakov, I.I. Strakovsky, and R.L. Workman, Phys Rev **C69** (2004) 035208 Z. Phys. **A359** (1997) 305

[18] M. Polyakov and A. Rathke, Eur. Phys. J. **A18** (2003) 691

[19] H.C. Kim, M. Polyakov, M. Praszalowicz, G.S. Yang, K. Goeke, (2005) hep-ph/0503237

[20] D.K. Hong, (2004) hep-ph/0412132

[21] V. Kuznetsov et al., Proceedings of the NSTAR2004 workshop on Excited Nucleons, March 2004, Grenoble, France; hep-ex/0409032

[22] R.A. Arndt, W.J. Briscoe, I.I. Strakovsky, and R.L. Workman, http://gwdac.phys.gwu.edu

[23] Y. Azimov, V. Kuznetsov, M. Polyakov, I. Strakovsky, (2005), hep-ph/0506236

[24] I. Jaegle, priv. com., preliminary results from the CBELSA/TAPS experiment,

[25] B. Krusche et al., LOI ELSA/2-2003

[26] A. Fix and H. Arenhövel, Z. Phys. **A359** (1997) 427.

[27] A. Fix and H. Arenhövel, Nucl. Phys. **A697** (2002) 277

[28] A. Sibirtsev et al., Phys. Rev. **C64** (2001) 024006.

[29] A. Sibirtsev et al., Phys. Rev. **C65** (2002) 044007.

[30] M. Martinez-Fabregate, PhD thesis, U. Mainz in preparation; P. Pedroni, priv. com.